



Technical Report
RAL-TR-95-051

Estimation of the Mixed Order Response Functions of Vector Non-linear Systems: Thermal Transport Processes

T Dewson and A D Irving

September 1995

© Council for the Central Laboratory of the Research Councils 1995

Enquiries about copyright, reproduction and requests for additional copies of this report should be addressed to:

The Central Laboratory for the Research Councils
Library and Information Services
Rutherford Appleton Laboratory
Chilton
Didcot
Oxfordshire
OX11 0QX
Tel: 01235 445384 Fax: 01235 446403
E-mail library@rl.ac.uk

ISSN 1358-6254

Neither the Council nor the Laboratory accept any responsibility for loss or damage arising from the use of information contained in any of their reports or in any communication about their tests or investigations.

ESTIMATION OF THE MIXED ORDER RESPONSE FUNCTIONS OF VECTOR NON-LINEAR SYSTEMS : THERMAL TRANSPORT PROCESSES

T Dewson

Department of Mathematics,
University of Bristol,
University Walk,
Bristol, BS8 1TW, UK.

AD Irving

Nonlinear Time Series Group,
Rutherford Appleton Laboratory,
Chilton, Didcot,
Oxon, OX11 0QX, UK.

Abstract

In this work a novel formalism to estimate the vector linear and leading non-linear impulse response functions from the experimental data observed from a multi-input system, allowing for correlation between the inputs, is presented. Time series statistical moments are estimated from the data and used as the basis of a set of simultaneous equations in the unknown response functions. These simultaneous equations are solved using standard matrix methods for the unknown response functions. The ability of the technique to correctly estimate the response functions of a multi-input non-linear system to a high degree of accuracy is demonstrated, using a numerical example where the properties of the system are known and there is strong correlation between the input data.

This novel technique is then used to estimate, from the time series, the first (linear) and second order response functions of the coupled convective and radiative processes, that act at the internal surface of the ceiling of a building. The estimated first and second order response functions all show discernible structure. The area / volume under the estimated response functions of each process are, respectively, the first and second order gains or heat transfer coefficients for that process. The response functions, of each process, estimated were employed to predict the surface heat flux, given the convective and radiative driving forces,

which could be compared with the measured heat flux.

The estimated linear heat transfer coefficients, from a vector mixed order analysis of the data, are compared with those obtained from a vector linear analysis of the same data. The first and second order response functions estimated by the novel technique from the time series all show discernible structure. This work will demonstrate whether the commonly used linear models of the convective and radiative processes are applicable.

Keywords

Time Series Analysis, Multi-Input Non-Linear Systems, Mixed Order Response Function Estimation, Time Series Moments.

Introduction

The analysis of time series data from dynamical systems is an important issue in numerous areas of science and engineering, and the study of linear systems has dominated scientific thinking for many years. A linear system has the property that the output produced is proportional to the input and that any complexity that arises may be described as the result of superposition. However in reality most, if not all, physical systems exhibit non-linear behaviour to some extent, and this makes them difficult to study. Thus there are few analysis techniques available to the experimentalist that can extract the relevant information, from the time series data, of a non-linear system, let alone one with multiple inputs where the inputs are correlated.

The most common tools employed for the analysis of time series data from linear systems are the linear correlation function and its Fourier transform, the spectral density. These tools are, respectively, applied in the least squares maximum likelihood estimation of a set parameters for an auto-regressive moving-average model, commonly known as the Box and Jenkins approach [1], and in the response function estimation technique in the frequency domain (for example, [2, 3]). Both these techniques are applied to the analysis of data from single input linear systems, and the frequency domain technique has been extended to estimate the linear and leading non-linear (2nd order) response functions for single-input [4] and multi-input systems [5].

Recently generalised theories for the estimation, in the time delay domain, of the impulse response functions of single-input mixed order (linear + non-linear) system [6] and of multi-input linear systems [7] have been developed. These techniques are based on the Volterra series, which is the generalisation of the linear convolution equation, and employs the statistical time delayed moments of the input and output time series in a characterisation of the system in terms of its impulse response functions. The impulse response function is a widely used means for the characterisation of a system (for example, [2, 3]).

In this paper, a new technique for the estimation of the linear and leading non-linear response functions of a multi-input system in the time domain is presented, which uses the same analysis formalism as developed and employed in the both single input non-linear [6]

and the multi-input linear [7] analyses techniques. That is, the use of the time delayed statistical moments between the input and output data.

The multi-input technique, developed in this work, will be applied to a non-linear analysis of this surface heat flux data, accounting for all the factors that affect the heat flux at the surface, i.e the convective, radiative and conductive processes, and the results obtained compared with those obtained from a multi-input linear analysis [7].

Estimation of the response functions of a multi-input non-linear system

In this section, a novel analysis technique for the estimation of the impulse response functions of a multi-input non-linear system, allowing for correlation between the inputs to the system, is presented. The response functions are used to characterise the properties of the system, in terms of it's physical observables. From this characterisation, inferences may be made about the properties of the system, in terms of physical laws, formulae, the form of the basis set, or the like. This characterisation, or identification of a model, of the physical system, given observations of the input and output time series data of the system, is thus an important problem in numerous areas of science.

The single-input single-output linear convolution equation, or it's equivalent in the frequency domain, is the most important input-output relationship for a linear system (for example, [2, 3]).

$$y(t) = \sum_{\tau=0}^{\mu} h_{yx}(\tau)x(t - \tau)$$

This can be extended to include non-linear terms, and is known as the Volterra series [8, 9].

$$y(t) = \sum_{\tau_1=0}^{\mu} h_{yx}(\tau_1)x(t - \tau_1) + \sum_{\tau_1=0}^{\mu} \sum_{\tau_2=0}^{\mu} h_{yxx}(\tau_1, \tau_2)x(t - \tau_1)x(t - \tau_2) + \dots$$

It conveys that the output of the system at the present time, t , $y(t)$, is dependant upon

the current (time, t) and previous (time, $t - \tau$) values of the input, $x(t)$ and $x(t - \tau)$, through a set of weighting or response functions, $h_{yx_i}(\tau_1)$ (linear or first order), $h_{yx_ix_j}(\tau_1, \tau_2)$ (second order), etc. That is the output has some 'memory' of length μ , of the previous values of the input time series. This equation can be extended to the multi-input case, where we will consider a system with N inputs and one output, from which the observed time series data is given by $x_i(t), i = 1, \dots, N$ for the inputs, and $y(t)$ for the output.

$$y(t) = \sum_{i=1}^N \sum_{\tau_1=0}^{\mu} h_{yx_i}(\tau_1) x_i(t - \tau_1) + \sum_{i=1}^N \sum_{j=i}^N \sum_{\tau_1=0}^{\mu} \sum_{\tau_2=0}^{\mu} h_{yx_ix_j}(\tau_1, \tau_2) x_i(t - \tau_1) x_j(t - \tau_2) \quad (1)$$

In this work we shall consider only up to the 2nd order case, i.e include only the 1st and 2nd order terms, as shown in equation (1). However the ideas presented are completely general and can be readily extended to arbitrary order. The technique is entirely novel, as there is no technique currently available for the analysis of multi-input non-linear systems in the time domain, though a technique exists for the analysis of two-input mixed first and second order systems in the frequency domain [5]. The techniques presented in this work are applicable to systems with an arbitrary number of inputs.

In the analysis of time series data, it is usual to draw on a number of assumptions, in developing a model of this system, when analysing the observed data. These are that the system is causal, time-invariant, has a finite length memory, and that the boundary conditions $x_i(t), i = 1, \dots, N$ and $y(t)$ are drawn from stationary stochastic sequences for which the second order time series moments exist.

As the boundary conditions are assumed to be drawn from stationary stochastic sequences, it is thus possible to use time series moments to characterise the response of the system, as an alternative to the multi-input convolution equation, given in equation (1). The authors have recently developed a formalism for the estimation of the linear and non-linear response functions of a mixed order system [6] and the estimation of the linear response functions of a multi-input linear system [7], involving the formation and solution of a set of simultaneous equations relating the time delayed moments between the input and output time series data. This formalism is adopted in this work, and used to develop a set of

simultaneous equations, from which the unknown response functions can be calculated.

The first equation in this set of simultaneous equations is formed by multiplying equation (1) by $x_p(t - \sigma_k)$, where σ_k denotes an arbitrary time delay and p denotes an arbitrary input channel, to give

$$\begin{aligned} x_p(t - \sigma_k)y(t) &= \sum_{i=1}^N \sum_{\tau_1=0}^{\mu} h_{yx_i}(\tau_1)x_p(t - \sigma_k)x_i(t - \tau_1) \\ &+ \sum_{i=1}^N \sum_{j=i}^N \sum_{\tau_1=0}^{\mu} \sum_{\tau_2=0}^{\mu} h_{yx_ix_j}(\tau_1, \tau_2)x_p(t - \sigma_k)x_i(t - \tau_1)x_j(t - \tau_2) \end{aligned}$$

By applying the expectation operator to this equation, we obtain

$$\begin{aligned} E[x_p(t - \sigma_k)y(t)] &= \sum_{i=1}^N \sum_{\tau_1=0}^{\mu} h_{yx_i}(\tau_1)E[x_p(t - \sigma_k)x_i(t - \tau_1)] \\ &+ \sum_{i=1}^N \sum_{j=i}^N \sum_{\tau_1=0}^{\mu} \sum_{\tau_2=0}^{\mu} h_{yx_ix_j}(\tau_1, \tau_2)E[x_p(t - \sigma_k)x_i(t - \tau_1)x_j(t - \tau_2)] \end{aligned} \quad (2)$$

This forms $N * (\mu + 1)$ equations, however we have $N * (\mu + 1) + \frac{1}{2}(N * (N + 1)) * (\mu + 1)^2$ unknowns, i.e the number of response function values. Hence we need to generate another $\frac{1}{2}(N * (N + 1)) * (\mu + 1)^2$ equations, to form a set of simultaneous equations which when solved yield the unknown response function values.

In order to form these equations it is necessary to multiply equation (1) by, $x_p(t - \sigma_k)x_q(t - \sigma_l)$ where σ_k and σ_l denote arbitrary time delays and p and q denote arbitrary input channels, to give

$$\begin{aligned} x_p(t - \sigma_k)x_q(t - \sigma_l)y(t) &= \\ &\sum_{i=1}^N \sum_{\tau_1=0}^{\mu} h_{yx_i}(\tau_1)x_p(t - \sigma_k)x_q(t - \sigma_l)x_i(t - \tau_1) \\ &+ \sum_{i=1}^N \sum_{j=i}^N \sum_{\tau_1=0}^{\mu} \sum_{\tau_2=0}^{\mu} h_{yx_ix_j}(\tau_1, \tau_2)x_p(t - \sigma_k)x_q(t - \sigma_l)x_i(t - \tau_1)x_j(t - \tau_2) \end{aligned}$$

By applying the expectation operator to this equation, we obtain

$$\begin{aligned}
E[x_p(t - \sigma_k)x_q(t - \sigma_l)y(t)] = & \\
& \sum_{i=1}^N \sum_{\tau_1=0}^{\mu} h_{yx_i}(\tau_1) E[x_p(t - \sigma_k)x_q(t - \sigma_l)x_i(t - \tau_1)] \\
& + \sum_{i=1}^N \sum_{j=i}^N \sum_{\tau_1=0}^{\mu} \sum_{\tau_2=0}^{\mu} h_{yx_i x_j}(\tau_1, \tau_2) E[x_p(t - \sigma_k)x_q(t - \sigma_l)x_i(t - \tau_1)x_j(t - \tau_2)]
\end{aligned} \tag{3}$$

Thus (2) and (3) together form a set of $N * (\mu + 1) + \frac{1}{2}(N * (N + 1)) * (\mu + 1)^2$ simultaneous equations which when solved by using standard matrix methods yield the unknown response function values.

The methodology presented here is quite general, and may be applied to a wide range of problems, we shall consider a specific application of the technique to the analysis of the heat transfer processes within buildings. However before we apply this novel technique to the analysis of real experimental data, we shall consider a numerical experiment with computer generated data, in which the properties of the system are known.

Numerical experiment using computer generated data

In this section, the results from a numerical experiment, where the properties of the linear multi-input system are known, are presented. A numerical experiment is used so that the accuracy and range of appropriate use of the technique in the estimation of the impulse response functions of a multi-input system can be assessed, through the comparison of the estimated, $h_{yx_i}(\tau_1)$, $h_{yx_i x_j}(\tau_1, \tau_2)$ and known, $g_{yx_i}(\tau_1)$, $g_{yx_i x_j}(\tau_1, \tau_2)$, response functions. This comparison will be performed on the basis of two statistical metrics, the root mean square and absolute mean differences between the known and estimated impulse response functions, where the root mean square difference, for the linear response functions, is given by,

$$\text{rms}_i = \sqrt{\left[\frac{1}{\mu + 1} \sum_{\tau_1=0}^{\mu} (h_{yx_i}(\tau_1) - g_{yx_i}(\tau_1))^2 \right]} \tag{4}$$

and the absolute mean difference by,

$$\text{abs diff}_i = \frac{1}{\mu + 1} \sum_{\tau_1=0}^{\mu} | (h_{yx_i}(\tau_1) - g_{yx_i}(\tau_1)) | \quad (5)$$

and for the non-linear response functions by,

$$\text{rms}_{ij} = \sqrt{\left[\frac{1}{(\mu + 1)^2} \sum_{\tau_1=0}^{\mu} \sum_{\tau_2=0}^{\mu} (h_{yx_ix_j}(\tau_1, \tau_2) - g_{yx_ix_j}(\tau_1, \tau_2))^2 \right]} \quad (6)$$

$$\text{abs diff}_{ij} = \frac{1}{(\mu + 1)^2} \sum_{\tau_1=0}^{\mu} \sum_{\tau_2=0}^{\mu} | (h_{yx_ix_j}(\tau_1, \tau_2) - g_{yx_ix_j}(\tau_1, \tau_2)) | \quad (7)$$

These two statistical metrics will demonstrate, whether or not, the technique can correctly estimate the known response functions to a high degree of accuracy.

In this example we use a three input - one output system, such that $N = 3$ in equation (1), and the known first and second order impulse response functions are given by,

$$\begin{aligned} g_{yx_1}(\tau_1) &= e^{-0.5 * (\frac{\tau_1 - 5}{3})^2} \\ g_{yx_2}(\tau_1) &= e^{-0.3\tau_1} * \cos(\pi * \tau_1 / 5) \\ g_{yx_3}(\tau_1) &= e^{-0.3\tau_1} \\ & \\ g_{yx_1x_1}(\tau_1, \tau_2) &= 0.0 \\ g_{yx_1x_2}(\tau_1, \tau_2) &= e^{-0.2\tau_1} * e^{-0.2\tau_2} \\ g_{yx_1x_3}(\tau_1, \tau_2) &= e^{-0.15\tau_1} * \cos(\pi * \tau_1 / 5) * e^{-0.15\tau_2} * \cos(\pi * \tau_2 / 5) \\ g_{yx_2x_2}(\tau_1, \tau_2) &= e^{-0.3\tau_1} * e^{-0.3\tau_2} \\ g_{yx_2x_3}(\tau_1, \tau_2) &= 0.0 \\ g_{yx_3x_3}(\tau_1, \tau_2) &= e^{-0.5 * (\frac{\tau_1 - 6}{4})^2} * e^{-0.5 * (\frac{\tau_2 - 6}{4})^2} \end{aligned} \quad (8)$$

Only 6 of the nine second order response functions are defined due to symmetry. The inputs to this system are taken from the experimentally measured time series values of the wind

speed, $ws(t)$, and heat flux at the internal surface of the ceiling, $q(t)$, from the data set described in the next section. The input time series for each of the first two channels of the system is convolved from the wind speed data, such that

$$x_1(t) = 0.5ws(t) + 0.75ws(t-1) + 0.6ws(t-2) + 0.55ws(t-3) + 0.5ws(t-4) + 0.43ws(t-5) + 0.4ws(t-6) + 0.35ws(t-7) + 0.3ws(t-8) + 0.2ws(t-9) + 0.15ws(t-10) + 0.1ws(t-11) + 0.05ws(t-12) - 0.05ws(t-13) - 0.1ws(t-14) - 0.15ws(t-15) - 0.2ws(t-16) - 0.1ws(t-17) - 0.05ws(t-18) - 0.05ws(t-19) - 0.03ws(t-20) - 0.01ws(t-21)$$

$$x_2(t) = 1.0ws(t) + 0.7ws(t-1) + 0.6ws(t-2) + 0.5ws(t-3) + 0.4ws(t-4) + 0.35ws(t-5) + 0.3ws(t-6) + 0.2ws(t-7) + 0.17ws(t-8) + 0.14ws(t-9) + 0.12ws(t-10) + 0.08ws(t-11) + 0.06ws(t-12) + 0.05ws(t-13) - 0.05ws(t-14) - 0.1ws(t-15) - 0.2ws(t-16) - 0.24ws(t-17) - 0.15ws(t-18) - 0.06ws(t-19) - 0.03ws(t-20) + 0.01ws(t-21)$$

Thus there will be a strong correlation between two of the input channels to the system. The input to the third channel is the unmodified surface heat flux time series data i.e $x_3(t) = q(t)$. The output data was generated using equation (1), with this input data and the known response functions given by equation (6), and the addition of a zero mean white noise sequence with an absolute mean of approximately 1% of the convolved signal.

The analysis is performed using 1000 points of time series data, and a maximum time delay of 20, i.e $\mu = 20$. [Note the area under a response function is given by $\sum_{\tau_1=0}^{\mu} h_{yx_i}(\tau_1)$ and $\sum_{\tau_1=0}^{\mu} \sum_{\tau_2}^{\mu} h_{yx_i x_j}(\tau_1, \tau_2)$].

Input Channel	Estimated Area	Theoretical Area	RMS difference	Absolute mean difference
1	7.2736401	7.2736336	$5.717 \cdot 10^{-7}$	$4.349 \cdot 10^{-7}$
2	1.1439284	1.1439354	$5.591 \cdot 10^{-7}$	$4.423 \cdot 10^{-7}$
3	3.8512109	3.8512109	$2.681 \cdot 10^{-11}$	$2.275 \cdot 10^{-11}$
1,1				
1,2				
1,3				
2,2				
2,3				
3,3				

Table 1: Results from the numerical experiment using computer generated data

The RMS and absolute mean differences of at least 10^{-7} demonstrate the ability and accuracy of this new technique. This example has demonstrated that the technique can correctly estimate the response functions of a multi-input system, even when two of the inputs to the system are highly correlated.

Experimental data

The experimental data set used in the present work was collected, from the British Gas plc test cell at Cranfield, by the Energy Monitoring Company (EMC), over the 1989/90 heating season [10]. The test cell has internal dimensions of 2.03m by 2.03m by 2.33m tall. The four walls of the test cell, which are of an externally insulated brick construction, are built off an insulated timber floor panel which has been raised on blocks above ground level, allowing the floor panel to be at the ambient external temperature. The flat roof of the test cell is of a timber-frame styrofoam construction, with waterproofed plywood as the external surface and plasterboard as the internal surface. The internal surfaces of the test cell are finished with a coat of matt white paint.

The test cell is exposed to natural external meteorological conditions, however no solar radiation is directly incident on any of the interior surfaces of the test cell. It is very highly sealed, as the natural infiltration rate was less than 0.05 ac/hr, as determined from a pressure test on the building [10]. The test cell was continuously mechanically ventilated by the outside air, ducted via a pulse output gas meter, to record the ventilation rate, which was set at approximately 2 ac/hr using dampers on the inlet and outlet ducts. This air entered the test cell via a diffuser pipe, running from the floor to the ceiling, in the north-west corner. The velocity in the diffuser pipe can be determined from the diameter of the pipe and the air change rate, and was approximately 0.7 m/s. The air, within the test cell, was heated by a 1 kW convective heater, controlled by a pseudo random sequence of on/off pulses with a 5 minute time step.

Time series data were collected at 5 minute intervals for a period of 20 days for the experiment. External meteorological measurements were obtained for the dry bulb temperature, wind speed and direction, and the global and diffuse horizontal irradiance. Internal

measurements were obtained for various air and surface temperatures, and for the heat flux at each surface. In order to estimate the surface heat transfer coefficient, a Meyer ladder [11] was employed, this measures the air temperature through the boundary layer, from the surface to which it is attached to the bulk air. A ladder consists of a set of air temperature sensors (in this case ten) at accurately defined distances from the surface, a free stream air temperature sensor, and a surface temperature sensor. In this experiment the ladder was mounted on the ceiling of the test cell in the proximity of the heat flux mat on this surface.

Application of technique

The new technique for the estimation of the response functions from multi-input systems presented in this work, will now be employed to investigate the energy balance at the surface of the ceiling in the test cell described in the previous section. The energy balance across a volume enclosing the surface can be written as,

$$q(t) = q_{conduction}(t) + q_{radiation}(t) + q_{convection}(t) \quad (9)$$

such that the observed heat flux at the surface, $q(t)$, is composed of components due to the conductive, radiative and convective processes that interact at the surface.

However, the construction of the test cell, i.e the layer of styrofoam on the external surface, means that the test cell has a time constant for the conductive path of the order of days, and so this path will be assumed to be negligible when compared with either the convective or radiative flowpaths. Hence equation (9) can be re-written as,

$$q(t) = q_{radiation}(t) + q_{convection}(t)$$

This equation can be written in terms of the physical observable variables and the response functions of each process, using equation (1) as,

$$q(t) = \sum_{\tau_1=0}^{\mu} h_{q\Delta T_r^4}(\tau_1)\sigma\Delta T_r^4(t - \tau_1) + \sum_{\tau_1=0}^{\mu} h_{q\Delta T_f}(\tau_1)\Delta T_f(t - \tau_1)$$

$$\begin{aligned}
& + \sum_{\tau_1=0}^{\mu} \sum_{\tau_2=0}^{\mu} h_{q\Delta T_r^4 \Delta T_r^4}(\tau_1, \tau_2) \sigma \Delta T_r^4(t - \tau_1) \sigma \Delta T_r^4(t - \tau_2) \\
& + \sum_{\tau_1=0}^{\mu} \sum_{\tau_2=0}^{\mu} h_{q\Delta T_f \Delta T_f}(\tau_1, \tau_2) \Delta T_f(t - \tau_1) \Delta T_f(t - \tau_2) \\
& + \sum_{\tau_1=0}^{\mu} \sum_{\tau_2=0}^{\mu} h_{q\Delta T_r^4 \Delta T_f}(\tau_1, \tau_2) \sigma \Delta T_r^4(t - \tau_1) \Delta T_f(t - \tau_2)
\end{aligned}$$

where $\{\Delta T_r^4(t), \Delta T_f(t)\}$ are, respectively, the temperature gradient within the ceiling, the difference between the fourth powers of the surface temperatures of the ceiling and the average of the remaining surfaces within the test cell, and the temperature difference across the air-surface boundary layer; $h_{q\Delta T_r^4}(\tau_1)$, $h_{q\Delta T_f}(\tau_1)$ are, respectively the linear response factors for the radiative and convective processes, and $h_{q\Delta T_r^4 q \Delta T_r^4}(\tau_1, \tau_2)$, $h_{q\Delta T_f q \Delta T_f}(\tau_1, \tau_2)$, $h_{q\Delta T_r^4 q \Delta T_f}(\tau_1, \tau_2)$ are the second order response factors of the radiative, convective and mixed radiative/convective processes. From this point in the work, the Stefan-Boltzmann constant, σ , will be combined with the difference between the fourth powers of the surface temperatures of the ceiling and the average of the remaining surfaces within the test cell, $\Delta T_r^4(t)$ and is equal to $56.7 * 10^{-9} \text{W/m}^2 \text{K}^4$. The cubic geometry of the test cell and the fact that all the surfaces within the test cell were finished with a coat of matt white paint mean that no account need be taken of the radiative view factors and the emissivity of each surface. The area under the estimated response factors for each process is the heat transfer coefficient or gain of that process [12].

Following the novel methodology presented in this work, we may take time series moments between the heat flux at the ceiling surface and the two temperature differences $\Delta T_r^4(t - \sigma_k)$, $\Delta T_f(t - \sigma_k)$, to give

$$\begin{aligned}
M_{\Delta T_r^4 q}(\sigma_k) & = \sum_{\tau_1=0}^{\mu} h_{q\Delta T_r^4}(\tau_1) M_{\Delta T_r^4 \Delta T_r^4}(\sigma_k, \tau_1) + \sum_{\tau_1=0}^{\mu} h_{q\Delta T_f}(\tau_1) M_{\Delta T_r^4 \Delta T_f}(\sigma_k, \tau_1) \\
& + \sum_{\tau_1=0}^{\mu} \sum_{\tau_2=0}^{\mu} h_{q\Delta T_r^4 \Delta T_r^4}(\tau_1, \tau_2) M_{\Delta T_r^4 \Delta T_r^4 \Delta T_r^4}(\sigma_k, \tau_1, \tau_2) \\
& + \sum_{\tau_1=0}^{\mu} \sum_{\tau_2=0}^{\mu} h_{q\Delta T_r^4 \Delta T_f}(\tau_1, \tau_2) M_{\Delta T_r^4 \Delta T_r^4 \Delta T_f}(\sigma_k, \tau_1, \tau_2) \\
& + \sum_{\tau_1=0}^{\mu} \sum_{\tau_2=0}^{\mu} h_{q\Delta T_f \Delta T_f}(\tau_1, \tau_2) M_{\Delta T_r^4 \Delta T_f \Delta T_f}(\sigma_k, \tau_1, \tau_2)
\end{aligned}$$

$$\begin{aligned}
M_{\Delta T_f q}(\sigma_k) &= \sum_{\tau_1=0}^{\mu} h_{q\Delta T_r^4}(\tau_1) M_{\Delta T_f \Delta T_r^4}(\sigma_k, \tau_1) + \sum_{\tau_1=0}^{\mu} h_{q\Delta T_f}(\tau_1) M_{\Delta T_f \Delta T_f}(\sigma_k, \tau_1) \\
&+ \sum_{\tau_1=0}^{\mu} \sum_{\tau_2=0}^{\mu} h_{q\Delta T_r^4 \Delta T_r^4}(\tau_1, \tau_2) M_{\Delta T_f \Delta T_r^4 \Delta T_r^4}(\sigma_k, \tau_1, \tau_2) \\
&+ \sum_{\tau_1=0}^{\mu} \sum_{\tau_2=0}^{\mu} h_{q\Delta T_r^4 \Delta T_f}(\tau_1, \tau_2) M_{\Delta T_f \Delta T_r^4 \Delta T_f}(\sigma_k, \tau_1, \tau_2) \\
&+ \sum_{\tau_1=0}^{\mu} \sum_{\tau_2=0}^{\mu} h_{q\Delta T_f \Delta T_f}(\tau_1, \tau_2) M_{\Delta T_f \Delta T_f \Delta T_f}(\sigma_k, \tau_1, \tau_2)
\end{aligned}$$

and the time series moments between the heat flux at the ceiling surface and all product combinations of the two temperature differences $\Delta T_f(t - \sigma_k) \Delta T_f(t - \sigma_l)$, $\Delta T_r^4(t - \sigma_k) \Delta T_f(t - \sigma_l)$, and $\Delta T_r^4(t - \sigma_k) \Delta T_r^4(t - \sigma_l)$ to give

$$\begin{aligned}
M_{\Delta T_r^4 \Delta T_r^4 q}(\sigma_k, \sigma_l) &= \sum_{\tau_1=0}^{\mu} h_{q\Delta T_r^4}(\tau_1) M_{\Delta T_r^4 \Delta T_r^4 \Delta T_r^4}(\sigma_k, \sigma_l, \tau_1) \\
&+ \sum_{\tau_1=0}^{\mu} h_{q\Delta T_f}(\tau_1) M_{\Delta T_r^4 \Delta T_r^4 \Delta T_f}(\sigma_k, \sigma_l, \tau_1) \\
&+ \sum_{\tau_1=0}^{\mu} \sum_{\tau_2=0}^{\mu} h_{q\Delta T_r^4 \Delta T_r^4}(\tau_1, \tau_2) M_{\Delta T_r^4 \Delta T_r^4 \Delta T_r^4 \Delta T_r^4}(\sigma_k, \sigma_l, \tau_1, \tau_2) \\
&+ \sum_{\tau_1=0}^{\mu} \sum_{\tau_2=0}^{\mu} h_{q\Delta T_r^4 \Delta T_f}(\tau_1, \tau_2) M_{\Delta T_r^4 \Delta T_r^4 \Delta T_r^4 \Delta T_f}(\sigma_k, \sigma_l, \tau_1, \tau_2) \\
&+ \sum_{\tau_1=0}^{\mu} \sum_{\tau_2=0}^{\mu} h_{q\Delta T_f \Delta T_f}(\tau_1, \tau_2) M_{\Delta T_r^4 \Delta T_r^4 \Delta T_f \Delta T_f}(\sigma_k, \sigma_l, \tau_1, \tau_2)
\end{aligned}$$

$$\begin{aligned}
M_{\Delta T_f \Delta T_r^4 q}(\sigma_k, \sigma_l) &= \sum_{\tau_1=0}^{\mu} h_{q\Delta T_r^4}(\tau_1) M_{\Delta T_f \Delta T_r^4 \Delta T_r^4}(\sigma_k, \sigma_l, \tau_1) \\
&+ \sum_{\tau_1=0}^{\mu} h_{q\Delta T_f}(\tau_1) M_{\Delta T_f \Delta T_r^4 \Delta T_f}(\sigma_k, \sigma_l, \tau_1) \\
&+ \sum_{\tau_1=0}^{\mu} \sum_{\tau_2=0}^{\mu} h_{q\Delta T_r^4 \Delta T_r^4}(\tau_1, \tau_2) M_{\Delta T_f \Delta T_r^4 \Delta T_r^4 \Delta T_r^4}(\sigma_k, \sigma_l, \tau_1, \tau_2) \\
&+ \sum_{\tau_1=0}^{\mu} \sum_{\tau_2=0}^{\mu} h_{q\Delta T_r^4 \Delta T_f}(\tau_1, \tau_2) M_{\Delta T_f \Delta T_r^4 \Delta T_r^4 \Delta T_f}(\sigma_k, \sigma_l, \tau_1, \tau_2) \\
&+ \sum_{\tau_1=0}^{\mu} \sum_{\tau_2=0}^{\mu} h_{q\Delta T_f \Delta T_f}(\tau_1, \tau_2) M_{\Delta T_f \Delta T_r^4 \Delta T_f \Delta T_f}(\sigma_k, \sigma_l, \tau_1, \tau_2)
\end{aligned}$$

$$\begin{aligned}
M_{\Delta T_f \Delta T_f q}(\sigma_k, \sigma_l) &= \sum_{\tau_1=0}^{\mu} h_{q \Delta T_f^4}(\tau_1) M_{\Delta T_f \Delta T_f \Delta T_f^4}(\sigma_k, \sigma_l, \tau_1) \\
&+ \sum_{\tau_1=0}^{\mu} h_{q \Delta T_f}(\tau_1) M_{\Delta T_f \Delta T_f \Delta T_f}(\sigma_k, \sigma_l, \tau_1) \\
&+ \sum_{\tau_1=0}^{\mu} \sum_{\tau_2=0}^{\mu} h_{q \Delta T_f^4 \Delta T_f^4}(\tau_1, \tau_2) M_{\Delta T_f \Delta T_f \Delta T_f^4 \Delta T_f^4}(\sigma_k, \sigma_l, \tau_1, \tau_2) \\
&+ \sum_{\tau_1=0}^{\mu} \sum_{\tau_2=0}^{\mu} h_{q \Delta T_f^4 \Delta T_f}(\tau_1, \tau_2) M_{\Delta T_f \Delta T_f \Delta T_f^4 \Delta T_f}(\sigma_k, \sigma_l, \tau_1, \tau_2) \\
&+ \sum_{\tau_1=0}^{\mu} \sum_{\tau_2=0}^{\mu} h_{q \Delta T_f \Delta T_f}(\tau_1, \tau_2) M_{\Delta T_f \Delta T_f \Delta T_f \Delta T_f}(\sigma_k, \sigma_l, \tau_1, \tau_2)
\end{aligned}$$

These five equations form a set of $3(\mu + 1) + 6(\mu + 1)^2$ simultaneous equations when σ_k and σ_l vary between 0 and μ , and is equal to the number of unknown response function values, taking account of symmetry in the second order response functions. These equations can be written in matrix form, and solved, for the unknown response functions, using standard matrix methods.

Analysis of experimental data

In this section the novel technique for the estimation of the first and second order impulse response functions of multi-input systems presented in this work, will be applied to the experimental data set previously described [10]. The first and second order response functions for the convective and radiative processes acting at the ceiling of the test cell will be estimated from the time series data. The first and second order convective and radiative heat transfer coefficients, for the ceiling of the test cell, will be determined, as the area / volume under the estimated response function are respectively the first and second order steady state gains of that process [12]. The first order steady state gain between the surface heat flux and the temperature difference driving force of a process is the first order convective heat transfer coefficient of that process [13]. The results from this multi-input mixed order analysis of the data will also be compared with those obtained from a multi-input linear analysis [7], and conclusions drawn regarding the necessity for the inclusion of all input variables to the appropriate order in the analysis of any process.

These estimated response functions characterise the convective and radiative processes that contribute to the observed heat flux, taking account of any correlation between the two processes. That is, the technique allows for the fact that one process may be 'driving' the other, hence the inputs are not strictly independent, if this is the case then the results from a single-input analysis may be questionable, as shown by the authors in previous work [7]. This technique allows an investigation to be performed on the order of the processes, through a comparison, of the relative magnitudes of the estimated first and second order surface heat transfer coefficients and, of the predictive power of the mixed order (linear / non-linear) estimator to that of the linear estimator [7], using the same sample of time series data.

Figure 1 shows a typical 24 hour sample of the temperature difference between a typical (the eighth) Meyer ladder sensor and the surface of the ceiling. Figure 2 shows the difference between the fourth powers of the surface temperature of the ceiling and the average temperature of the remaining surfaces within the test cell, allowing for the Stefan-Boltzmann constant, for the same 24 hour period. Figure 3 shows the corresponding 24 hour sample of the heat flux at the ceiling surface, shown as positive with heat flow into the surface.

The response functions for the convective and radiative processes, from which the convective and radiative heat transfer coefficients are determined, were estimated from a sequence of 1440 points (i.e 5 days) of time series data, for each of the ten Meyer ladder sensors. The maximum length of time delay or the length of the memory of the processes, μ , was set to 1 hour (i.e 12 points). Table 2 presents the first order convective and radiative heat transfer coefficients estimated for each Meyer ladder sensor, calculated as the area under the estimated first order response function for each process at each Meyer ladder sensor.

This table shows that the novel technique, presented in this work, produces consistent estimates of the radiative heat transfer coefficient across the air-ceiling boundary layer, and that as in previous analyses [7, 13], the estimated convective heat transfer coefficients vary across the boundary layer, but outside the boundary layer are consistent. Previous analysis has shown that the air-ceiling boundary layer is approximately 50 mm thick, and that the edge is between the fourth and fifth Meyer ladder sensors [7]. A comparison of these first order convective and radiative heat transfer coefficients with those obtained from the multi-

input linear analysis of the same data, show that the convective heat transfer coefficient is approximately the same in the two cases, whereas the estimate of the radiative heat transfer coefficient has increased by approximately 50%.

Sensor Number	Convective HTC (W/m^2K)	Radiative HTC
1	8.260	0.582
2	6.691	0.630
3	5.864	0.631
4	6.058	0.607
5	4.088	0.536
6	3.636	0.507
7	3.281	0.531
8	3.284	0.535
9	3.271	0.579
10	3.287	0.564

Table 2: First order Convective and Radiative heat transfer coefficients for each Meyer ladder sensor, from the multi-input approach

Table 3 presents the second order convective, radiative and mixed convective / radiative heat transfer coefficients estimated for each Meyer ladder sensor, calculated as the volume under the estimated second order response function for each process at each Meyer ladder sensor.

Sensor Number	Convective HTC (W/m^2K)	Mixed Conv / Rad HTC	Radiative HTC
1	1.494	-0.450	$-1.48 \cdot 10^{-2}$
2	$-8.33 \cdot 10^{-3}$	-0.414	$-2.0 \cdot 10^{-2}$
3	-0.371	-0.336	$-1.90 \cdot 10^{-2}$
4	-0.762	-0.296	$-1.85 \cdot 10^{-2}$
5	0.225	-0.109	$-7.13 \cdot 10^{-3}$
6	0.344	$-7.13 \cdot 10^{-2}$	$-4.48 \cdot 10^{-3}$
7	0.362	$-7.12 \cdot 10^{-2}$	$-2.02 \cdot 10^{-3}$
8	0.278	$-6.94 \cdot 10^{-2}$	$-4.36 \cdot 10^{-3}$
9	0.220	-0.132	$-5.18 \cdot 10^{-3}$
10	0.245	-0.117	$-5.53 \cdot 10^{-3}$

Table 3: Second order Convective and Radiative heat transfer coefficients for each Meyer ladder sensor, from the multi-input approach

This table shows that the novel technique, presented in this work, produces estimated second order radiative heat transfer coefficients that are again consistent over the air-ceiling boundary layer, but are approximately 100 times smaller than the first order estimates, which when one takes into account the magnitude of the input time series, i.e the difference between the fourth powers of the surface temperature of the ceiling and the average temperature of the remaining surfaces within the test cell, means that the linear component of the estimated radiative heat flux will be approximately about 95% of the total, implying that the linear ΔT_r^4 representation of the radiative process is a good model. The estimated second order convective heat transfer coefficient are again consistent outside the air-ceiling boundary layer, and are approximately 10 times smaller than the first order estimates, which means that the linear component of the estimated convective heat flux will be approximately only about 80% of the total, implying that the linear ΔT_f representation of the convective process is not as good a model as the radiative one.

Figure 4 shows the estimated linear / first order response function of the surface heat flux to the temperature difference between the eighth Meyer ladder sensor and the surface of the ceiling. The area under this curve is the first order convective heat transfer coefficient between the ceiling and the air around the eighth sensor, and is $3.28W/m^2K$. Figure 5 shows the corresponding estimated linear response function of the surface heat flux to the difference between the fourth powers of the surface temperature of the ceiling and the average temperature of the remaining surfaces. The area under this curve is the radiative heat transfer coefficient, which for the eight Meyer ladder sensor is 0.53.

Figure 6 shows the estimated second order response function of the surface heat flux to the temperature difference between the eighth Meyer ladder sensor and the surface of the ceiling. It can be observed from this figure that there is structure in the estimated second order convective response function down the $\tau_1 = \tau_2$ diagonal. (Note that the axes on this figure are negative in the upward direction). The volume under this surface is the second order convective heat transfer coefficient between the ceiling and the air around the eighth sensor, and is $0.278W/m^2K$. Figures 7 and 8 show the estimated response functions for the radiative and mixed convective / radiative processes respectively. Again both these figures show structure, as in figure 6.

By using the estimated response functions of the convective and radiative processes and 3 hours of the driving forces, away from the 5 day sample chosen to perform the analysis, the predicted surface heat flux was estimated. Figure 9 shows the measured and predicted surface heat flux, and an excellent agreement can be observed, especially noting that the prediction region is away from the region used for the data analysis. A comparison with prediction obtained from the multi-input linear analysis of the same data [7], shows an improvement even on the excellent prediction by the linear technique. This excellent prediction can be more clearly observed if the predicted surface heat flux value is plotted against the corresponding measured surface heat flux value, as is shown in figure 10, the straight line through the origin with little dispersion demonstrates the excellent model of the system provided by the estimated first and second order response functions, which have been calculated from the time series data of the system. Figure 11 shows the predicted heat flux, as shown in figure 9, split into its convective, radiative and mixed convective/radiative components, as calculated from the estimated response functions. This figure shows that the combined first and second order convective process is driving heat into the ceiling surface, whereas the combined radiative and the second order mixed convective / radiative processes are usually removing heat from ceiling. The balance being that usually the heat transfer due to the convective process is larger than the sum of the other two.

Conclusions

A new technique for the estimation of the vector mixed order response functions from the time series of a multi-input non-linear system, that allows for correlation between the time series inputs has been presented. The technique is a time series method, and is based upon the observed correlation between the experimentally observed values and the impulse response functions, which are characterisations of the physical relationships between the input-output variables. The ability of this novel technique to correctly estimate the response functions of a multi-input non-linear system is demonstrated, using a numerical example. In this numerical example, where the properties of the system are known, the technique is shown to estimate the response functions of the system to a high degree of accuracy.

The technique is then applied to analyse time series data collected from a well insulated, single zone experimental building. The technique is employed to estimate the response functions of the coupled convective / radiative processes that act at the internal surface of the ceiling of the building. The area under the estimated response function of each process is the heat transfer coefficient of that process. These show the first order convective heat transfer coefficient between the ceiling surface and the bulk air within the single zone building to be approximately $3.2W/m^2K$, and the first order radiative heat transfer coefficient between the ceiling surface and the other surfaces within the zone to be approximately 0.55 . These values agree well with currently used empirical ones.

The form of the estimated first order response function of each process has demonstrated that both the convective and radiative processes acting at an internal surface have a short term 'memory' of about 10 minutes. That is the heat flux, at the current time, is predominantly (given that the major contribution to the estimated surface heat flux by the convective and radiative process are from the first order terms) affected by the convective and radiative driving forces of up to 10 minutes ago.

The form of the estimated second order response functions for the convective, radiative and mixed convective / radiative processes show structure, especially along the $\tau_1 = \tau_2$ diagonal. The estimated second order radiative heat transfer coefficient was shown to be approximately 100 times smaller than the estimated first order one, which means after taking into account the magnitude of the input time series, means that the linear component of the estimated radiative heat flux will be approximately about 95% of the total, implying that the linear ΔT_r^4 representation of the radiative process is a good model. The estimated second order convective heat transfer coefficient are consistent outside the air-ceiling boundary layer, and are approximately 10 times smaller than the first order estimates, which means that the linear component of the estimated convective heat flux will be approximately only about 80% the convective process is not as good a model as the radiative one.

The response functions and heat transfer coefficients estimated by the multi-input mixed order approach, presented in this paper, were compared with those obtained from a multi-input linear approach (from [7]). This comparison showed that the estimated first order response functions obtained in both cases, were similar in form, and that the convective and

radiative heat transfer coefficients, determined from these estimated response functions, were within 10% in of each other in the convective case, but in the radiative case a 50% difference was observed. However the estimated heat transfer coefficients were consistent, between the two cases, across the boundary layer.

Acknowledgments

The authors would like to express their thanks to the Energy Monitoring Company who collected and supplied the field data, and to British Gas Plc who funded the data collection.

References

- [1] Box GEP and Jenkins GM, Time Series Analysis - Forecasting and Control, Holden-Day, San Francisco, 1976.
- [2] Priestley MB, Spectral Analysis and Time Series, Academic Press, London, 1981.
- [3] Newland DE, An introduction to Random Vibrations and Spectral Analysis, Longman, London, 1975.
- [4] Kim KI and Powers EJ, A Digital Method of Modelling Quadratically Non-Linear Systems with a General Random Input, IEEE Trans. Acoust., Speech, Signal Processing, Vol 36 no. 12, 1988.
- [5] An CK, Powers EJ and Ritz CP, A Digital Method of Modelling Two-Input Quadratic Systems with General Random Inputs, IEEE Trans. Signal Processing, Vol 39 No. 10, 1991.
- [6] Irving AD; Dewson T, Hong G and Cunliffe N, Generalised Response of a Non-Linear System to Stochastic Sequences, Accepted Applied Mathematical Modelling, July 1994 [also Rutherford Appleton Laboratory report RAL-91-067].
- [7] Dewson T and Irving AD, Response Function Estimation from Multi-Input Systems, Accepted Applied Mathematical Modelling, September 1994.
- [8] Volterra V, Theory of Functionals and of Integral and Integro-Differential Equations, Dover, New York, 1959.
- [9] Schetzen M, The Wiener and Volterra Theories of Non-Linear Systems, John Wiley, New York, 1980.

- [10] Martin C and Watson M, Further Experiments in a Highly Instrumented Test Room, Energy Monitoring Company report and data set, Private communication, 1990.
- [11] Delaforce S, Hitchin ER and Watson M, Private communication, 1992.
- [12] Irving AD, Stochastic Sensitivity Analysis, Applied Mathematical Modelling 16, 1992.
- [13] Irving AD, Dewson T and Day B, Time Series Estimation of Convective Heat Transfer Coefficients, Building and Environment, Vol 28 No. 2, 1993

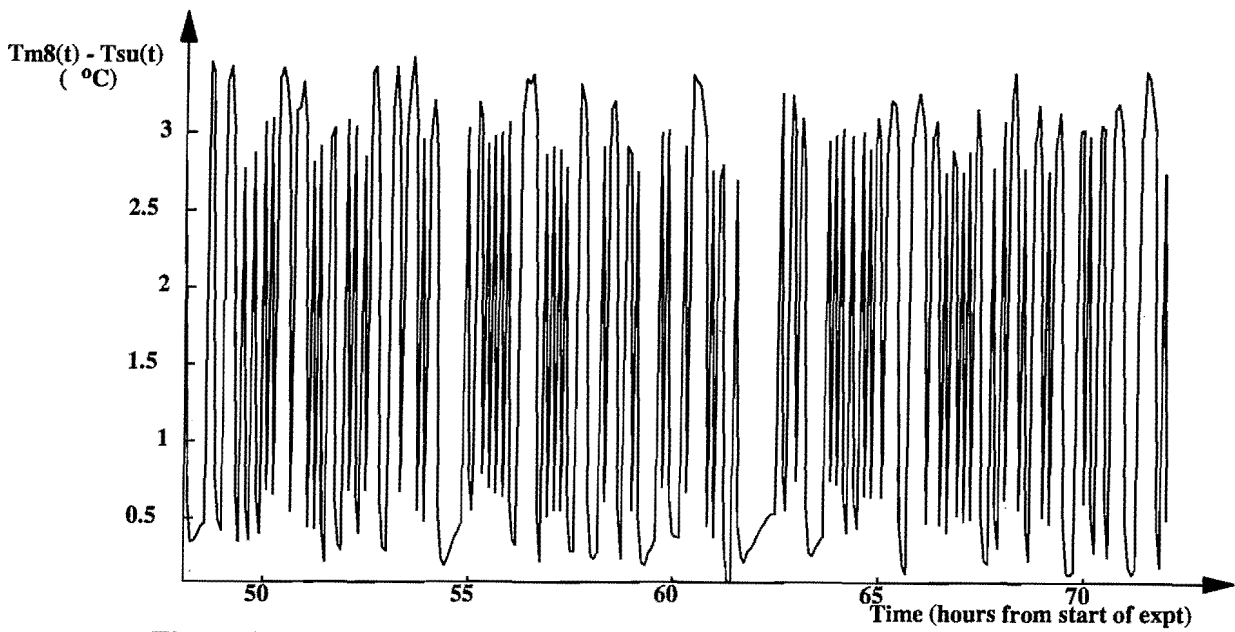


Figure 1 : A typical 24 hour sample of the temperature difference between the eighth Meyer ladder sensor and the surface of the ceiling

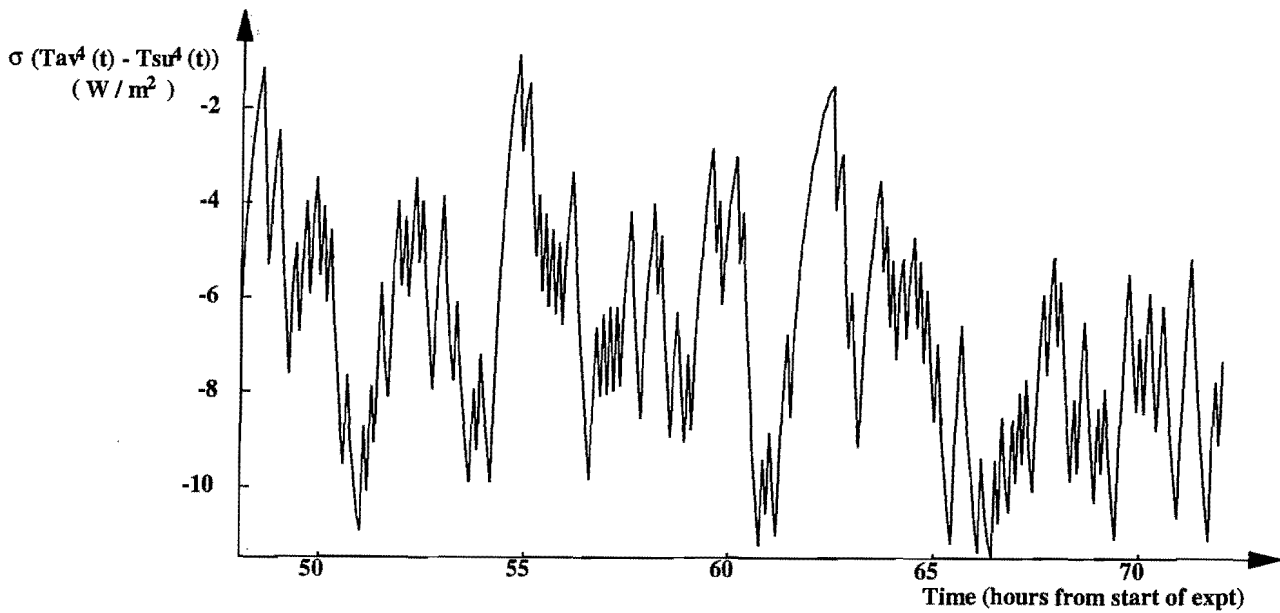


Figure 2 : A typical 24 hour sample of the difference between the fourth powers of the temperatures of the ceiling surface and average of the remaining surfaces

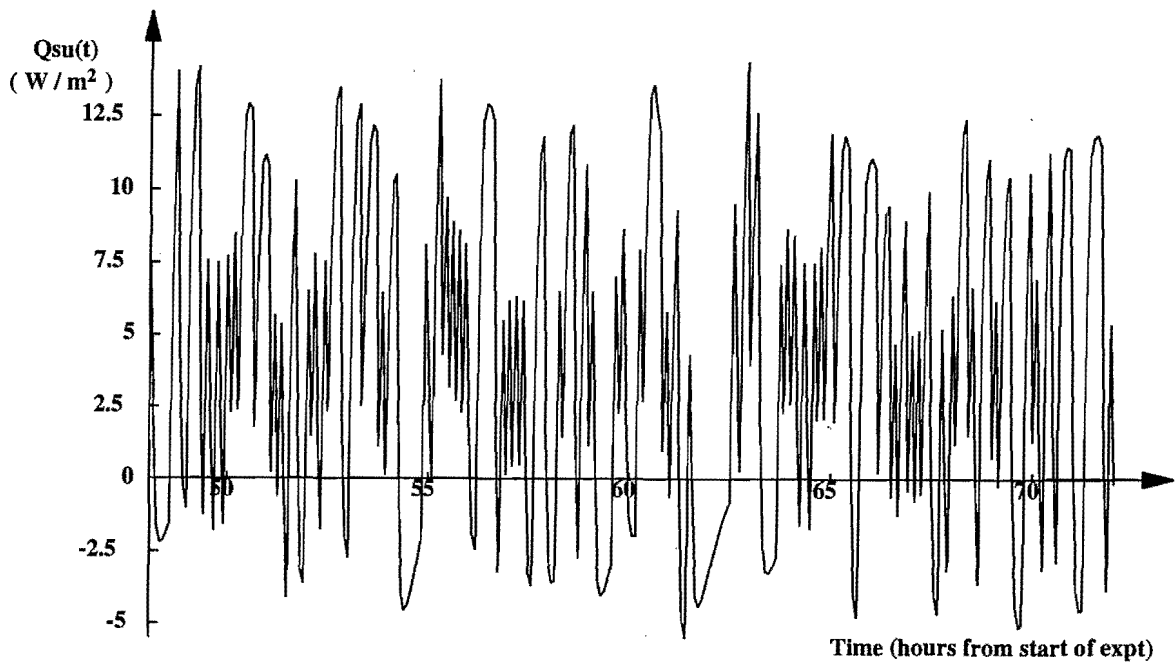


Figure 3 : A typical 24 hour sample of the heat flux at the ceiling surface

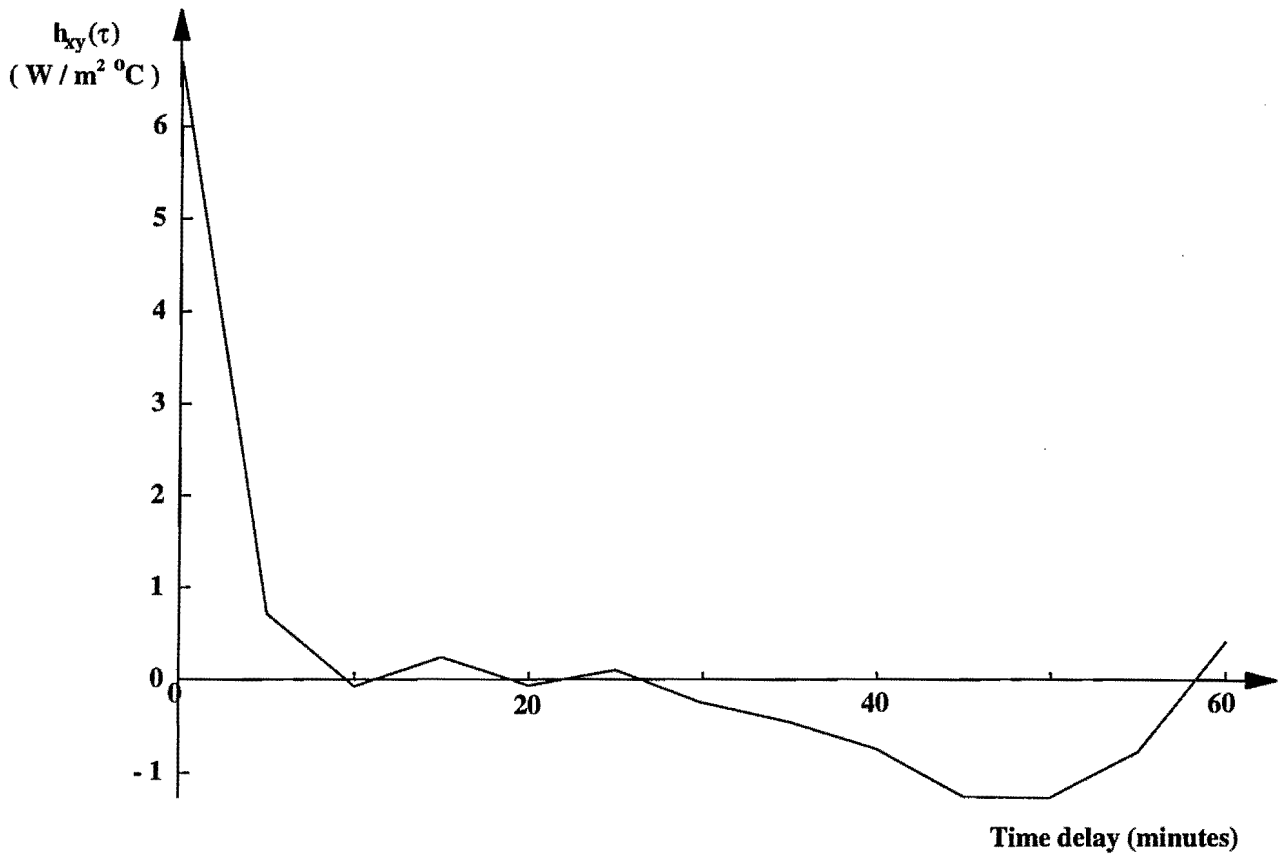


Figure 4 : Estimated linear response function of the surface heat flux to the temperature difference between the eighth ladder sensor and the ceiling surface (The first order response function of the convective process)

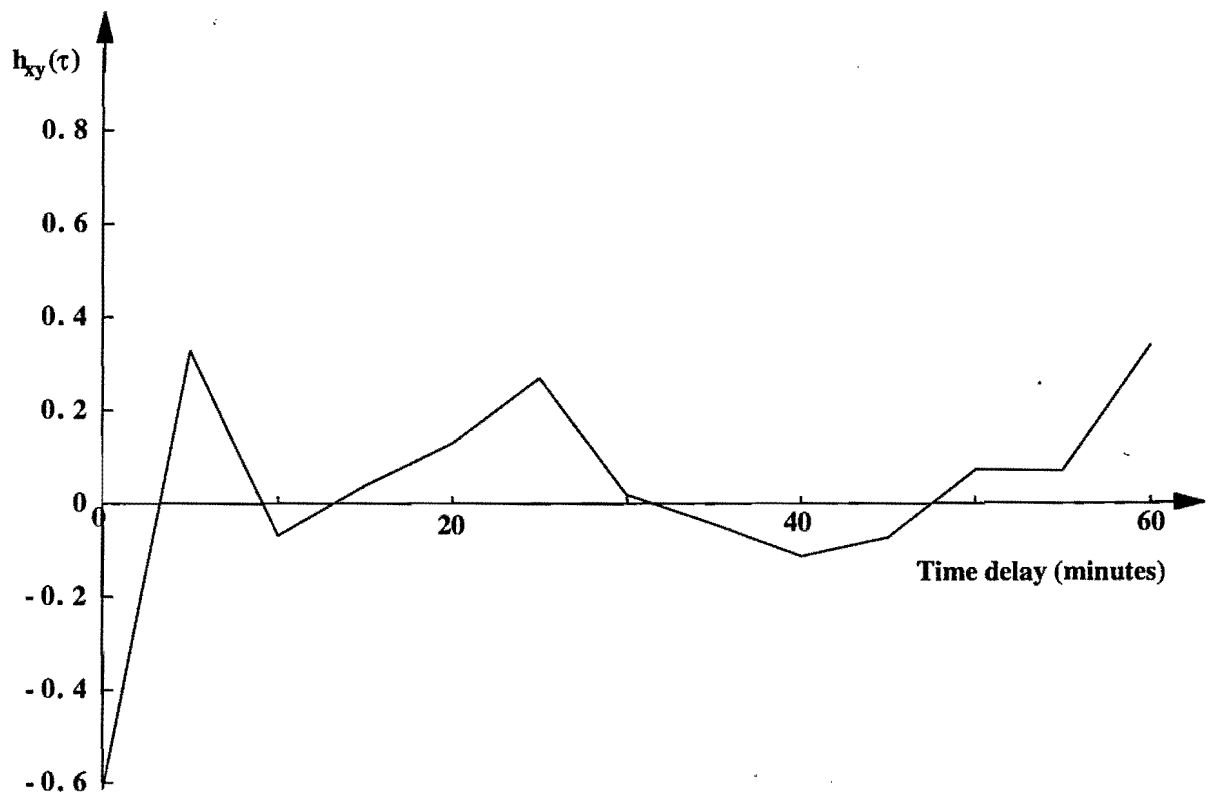


Figure 5 : Estimated linear response function of the surface heat flux to the difference between the fourth powers of the surface temperatures (The first order response function of the radiative process)

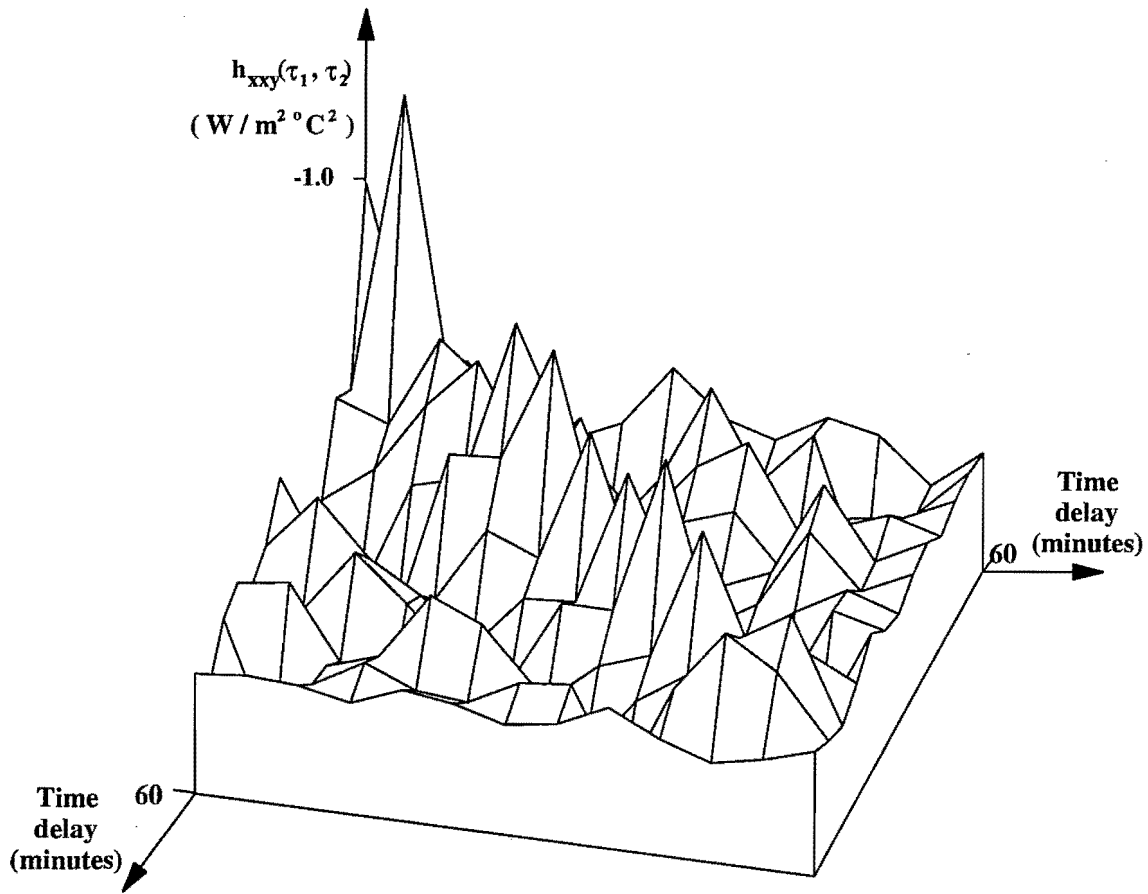


Figure 6 : Estimated second order response function of the surface heat flux to the temperature difference between the eighth ladder sensor and the ceiling surface (The second order response function of the convective process)

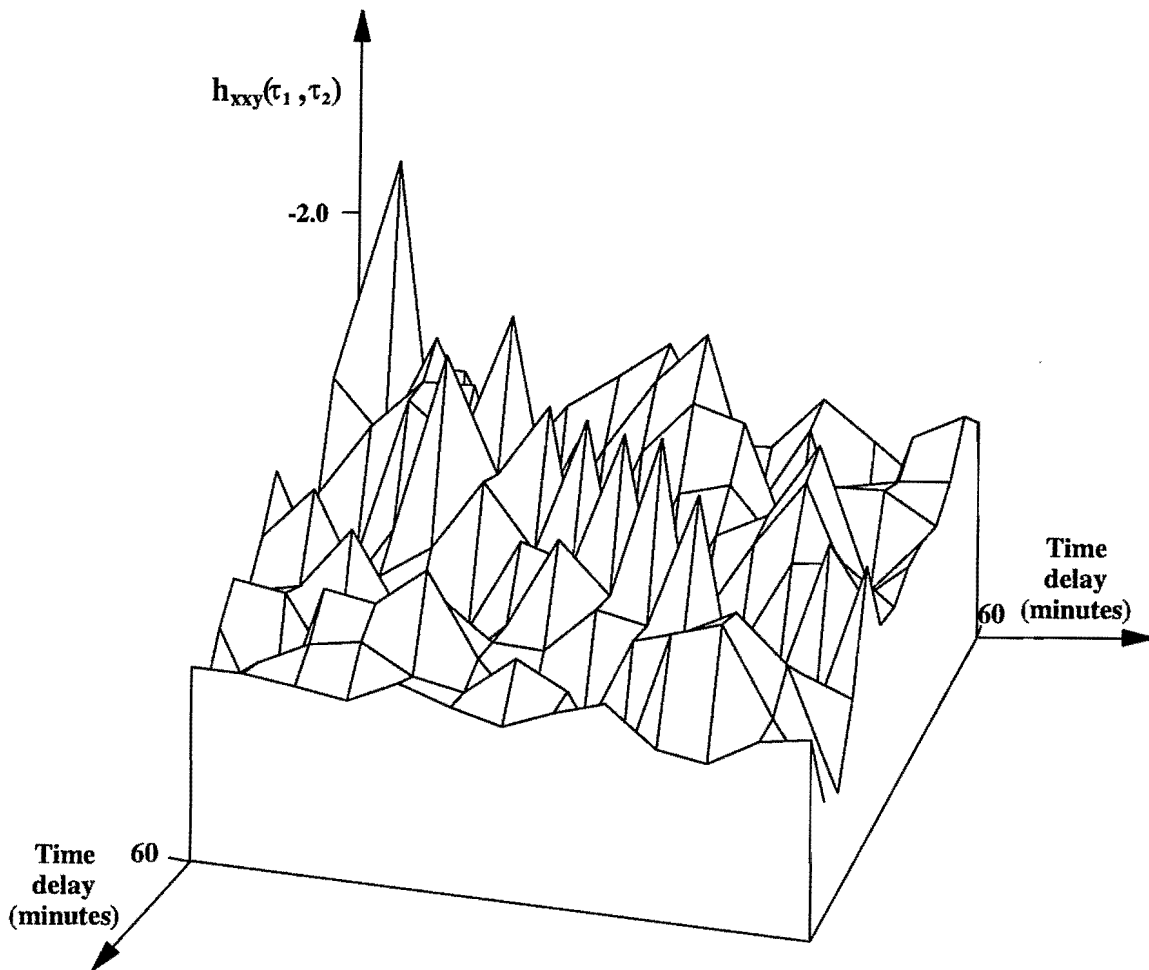


Figure 7 : Estimated second order response function of the surface heat flux to the difference between the fourth powers of the surface temperatures and the temperature difference between the ceiling surface and the ladder sensor (The second order response function of the mixed convective / radiative process)

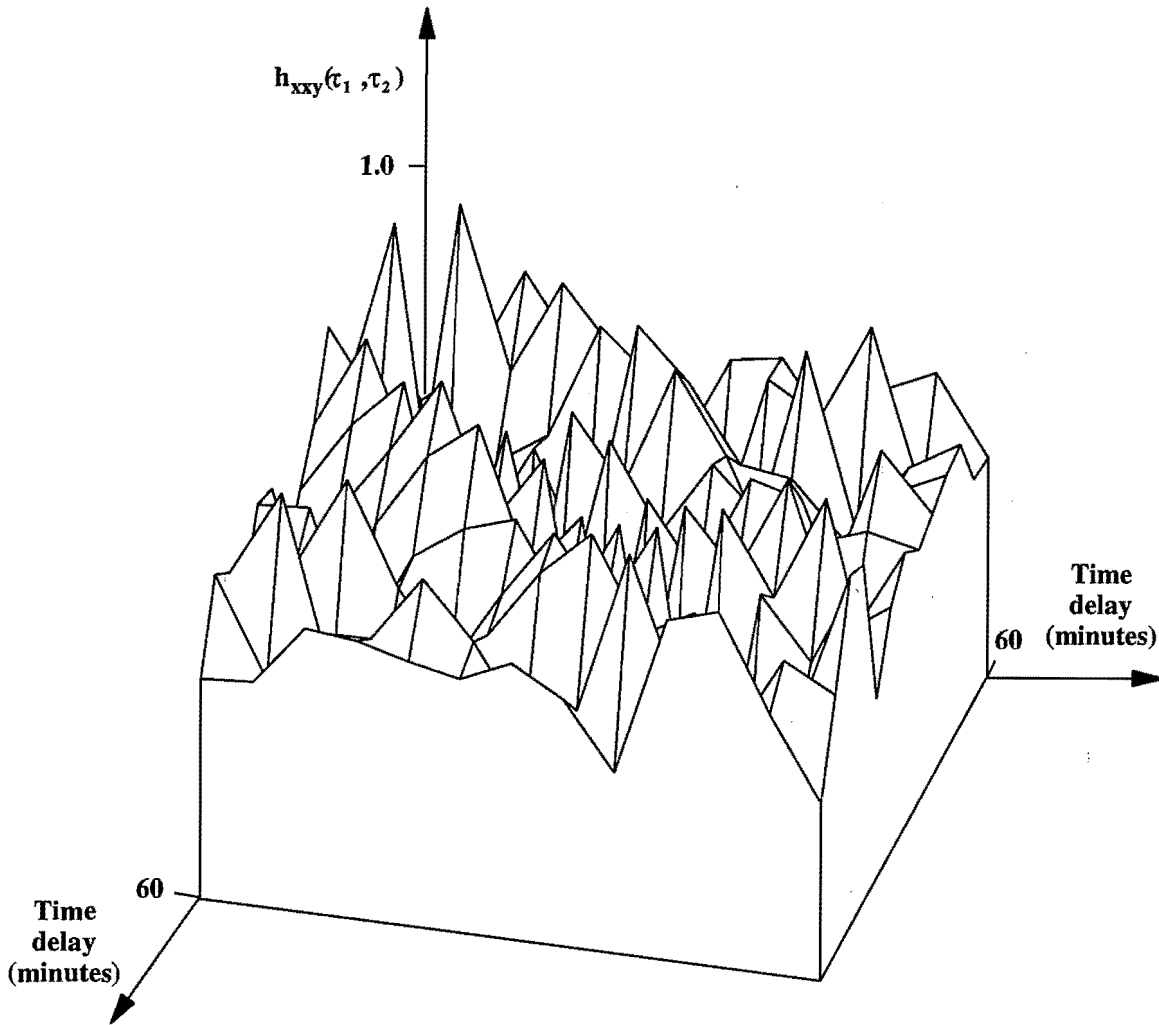


Figure 8 : Estimated second order response function of the surface heat flux to the difference between the fourth powers of the surface temperatures (The second order response function of the radiative process)

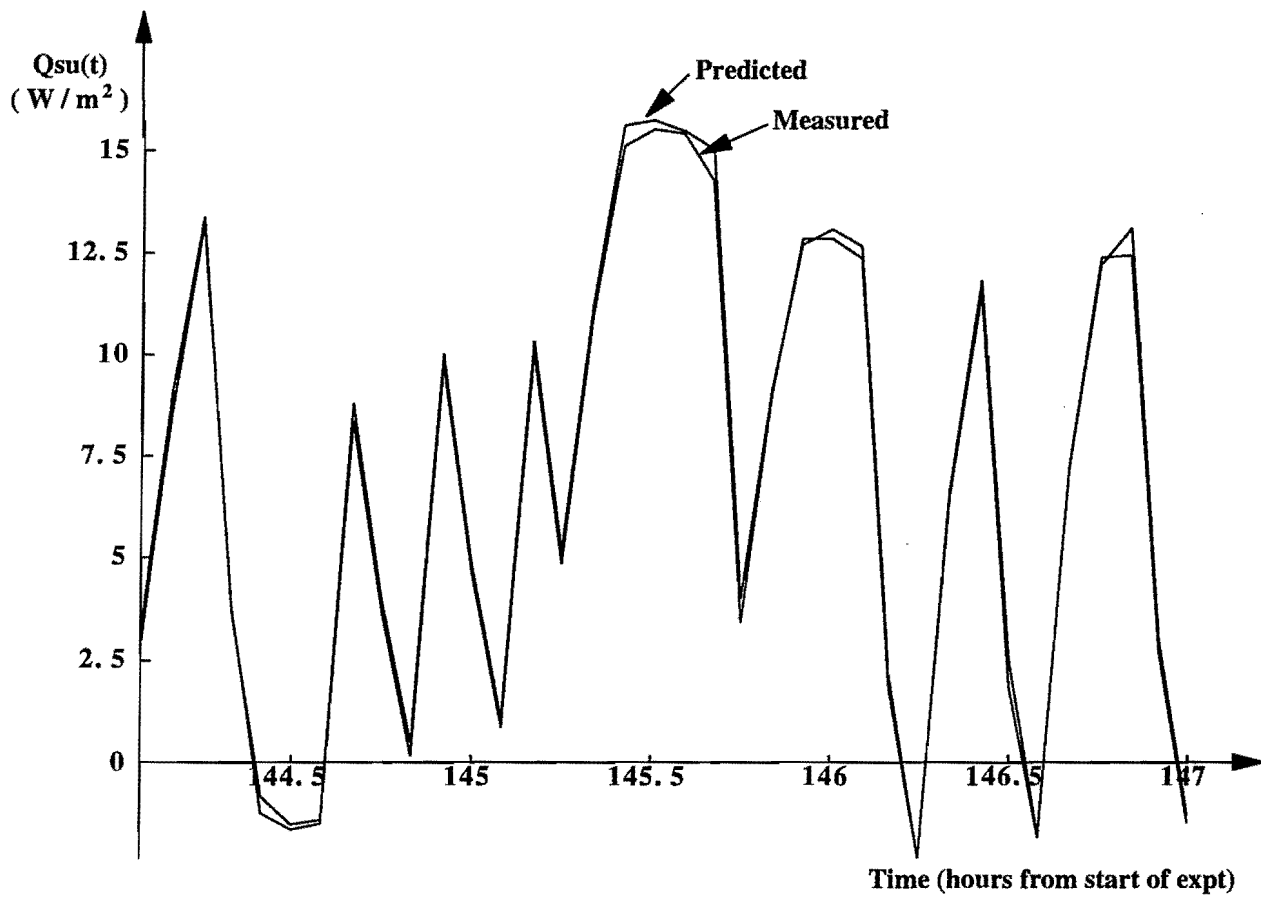


Figure 9 : A sample of the measured and predicted (using the convective and radiative response functions estimated by the multi-input formalism) heat flux at the surface of the ceiling

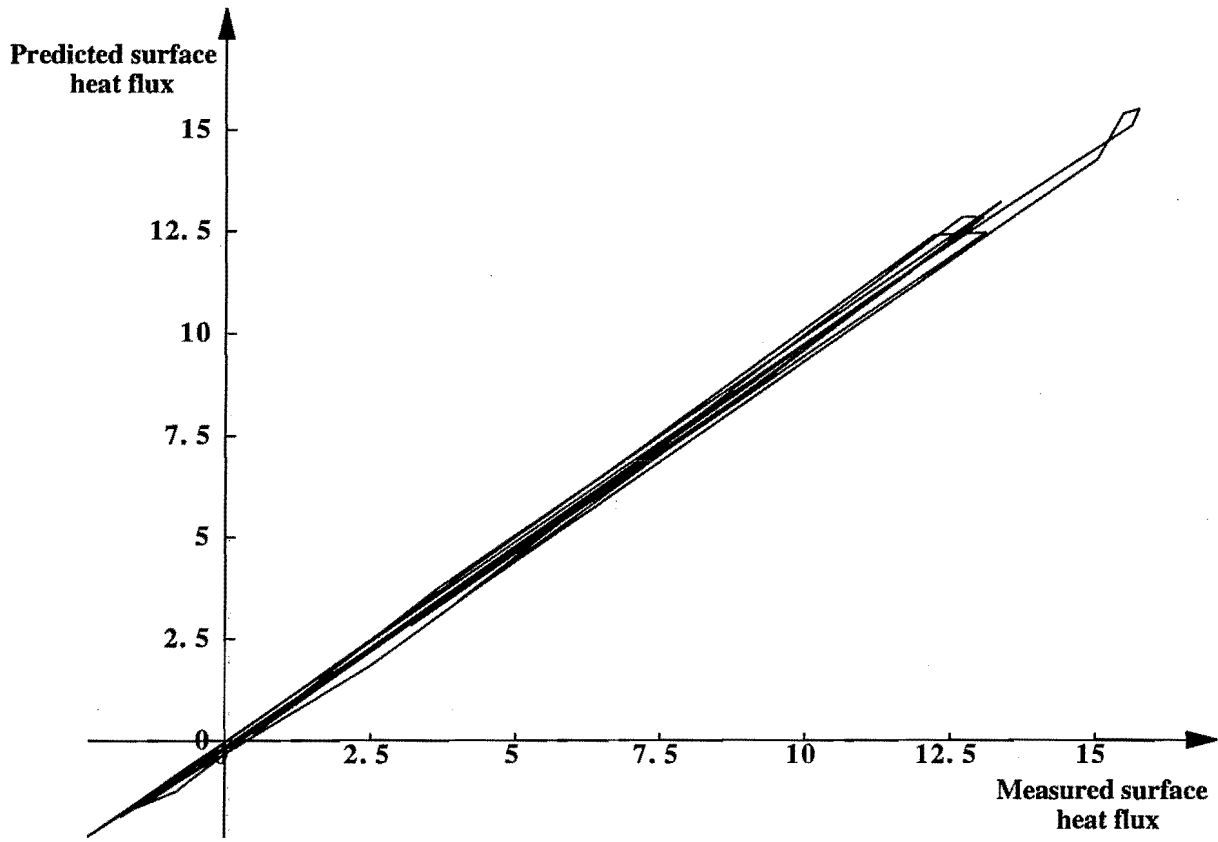


Figure 10 : A sample of the predicted (using the estimated response functions) surface heat flux plotted against the corresponding measured surface heat flux

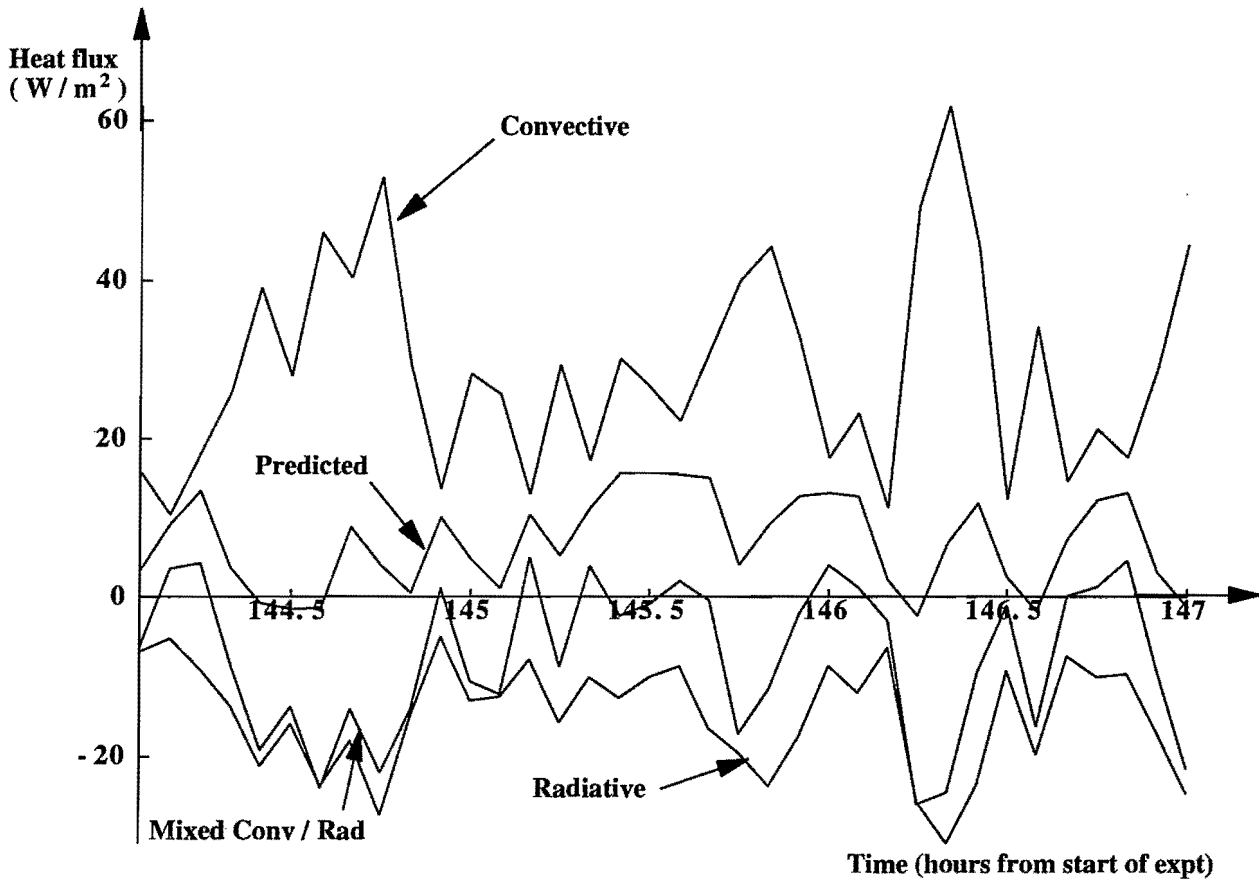


Figure 11 : A sample of the predicted heat flux at the ceiling surface, split into it's convective and radiative components, as predicted from the convective radiative, mixed convective / radiative response functions estimated by the multi-input mixed order formalism

